Cell Reports

Supplemental Information

Rad53-Mediated Regulation of Rrm3 and Pif1 DNA Helicases Contributes to Prevention of Aberrant Fork Transitions under Replication Stress

Silvia Emma Rossi, Arta Ajazi, Walter Carotenuto, Marco Foiani, and Michele Giannattasio

Supplemental information

Supplemental data

Rossi et al. Supplemental Figure S1

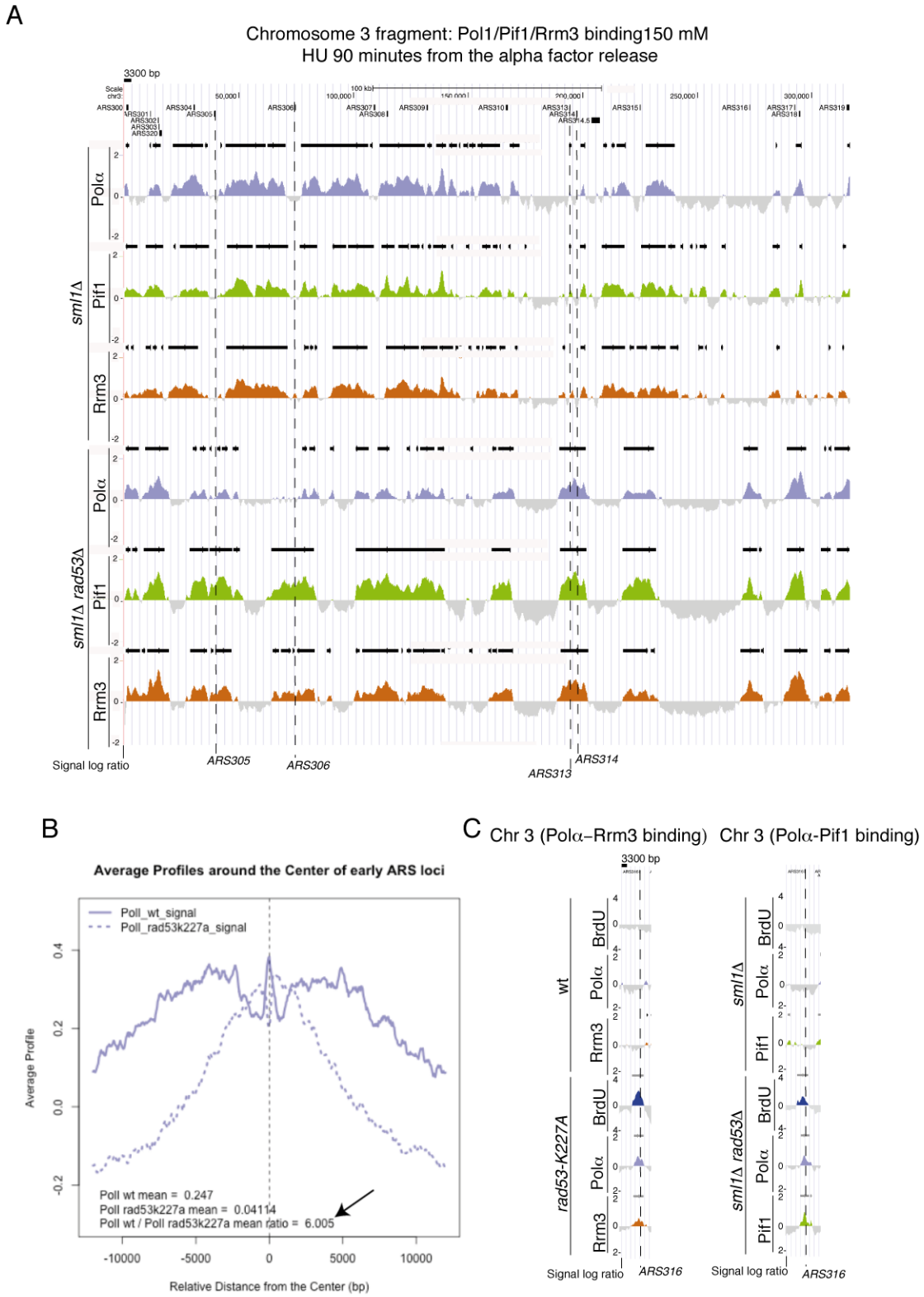

Figure S1. Rrm3 and Pif1 are replisome components under replication stress and are recruited at the late origin *ARS316*, which is fired in HU in the absence of Rad53 (related to Figure 1). A) Rrm3 and Pif1 are replisome components under replication stress. Polα-Flag (light blue), Pif1-Flag (green) and Rrm3-13Myc (red) binding profiles were determined by ChIP on chip in CY13284, CY13282, CY13074, CY13073, CY12470 and CY12422 strains, released from G1 into 150 mM of HU for 90 minutes. The y-axis show the enrichment signals expressed as ratio log2 IP/SUP of *loci* significantly enriched in the IP fractions. The horizontal black bars indicate statistically significative binding clusters. X-axis represents chromosomal coordinates. Early (*ARS305* and *ARS306*) and dormant origins (*ARS313* and *ARS314*) are marked by dashed black lines. The space between two light blue lines in the chromosome map corresponds to 3,3 kbp. **B) DNA polymerase alpha binding to flanking regions of 141 active *ARSs* is reduced in *rad53* mutants treated with high HU doses**. The area below the profiles showed in the first plot in the main figure 1C of the manuscript has been measured. The area values measured are directly linked to the magnitude of DNA polymerase alpha binding to 141 *ARSs* in the indicated genetic background. A black arrow indicates the ratio of DNA Polymerase alpha binding in wild type vs *rad53-K227A* cells in the indicated experimental condition. As it may be noticed DNA polymerase alpha binds 6 times less in *rad53-K227A* compared to wild type cells to 141 active *ARSs*. **C)** Binding profiles (enrichment signal log2 IP/SUP ratio) of Polα (light blue), Pif1 (light green), Rrm3 (red), determined by ChIP on chip and BrdU incorporation profiles (dark blue) determined by ssDNA-BrdU IP on chip (enrichment signal log2 IP/SUP ratio), in the same experiments of Figure 1A-B are

shown.

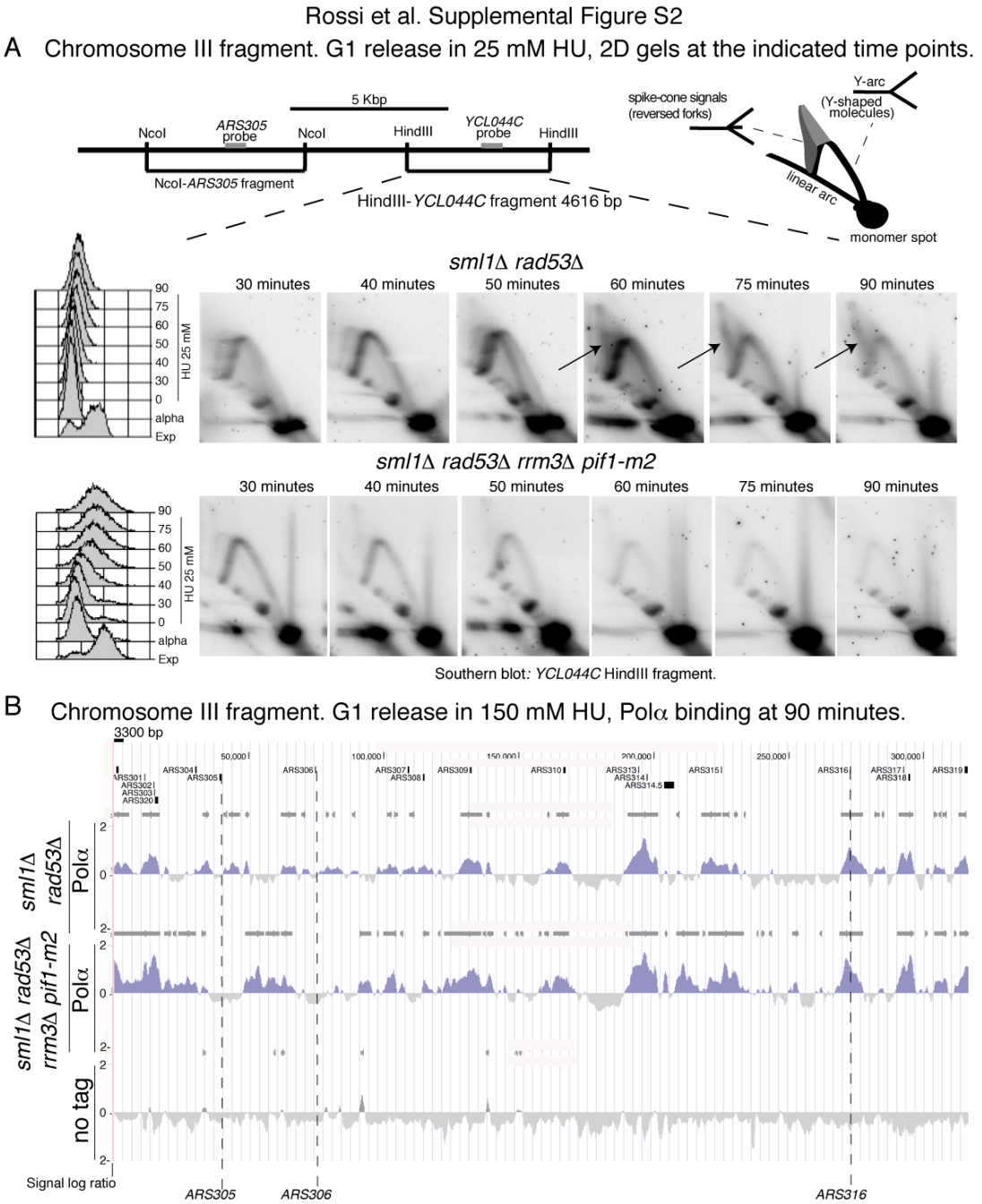

Figure S2. Rrm3 and Pif1 promote fork stalling and fork reversal in *rad53* mutants under replication stress, (related to Figure 2).

A) The strains *sml1Δ rad53Δ* (CY12443) and *sml1Δ rad53Δ rrm3Δ pif1-m2* (CY13342) have been synchronized in G1 and released into the cell cycle in the presence of 25 mM of HU. DNA replication intermediates (accumulating on the HindIII-*YCL044C* fragment schematically represented in the figure), have been analyzed by neutral-neutral 2D gels on *in-vivo* psoralen cross-linked genomic DNA at the indicated time points. FACS profiles showing the cellular DNA contents during

the experiment are reported. A schematic representation of the 2D gel signals detected in these experimental conditions is shown. Black arrows indicate the accumulation of the spike/cone signal, which represents the reversed forks, which accumulate in *rad53* cells under replication stress. **B)** The strains *sml1Δ rad53Δ* (CY13282), *sml1Δ rad53Δ rrm3Δ pif1-m2* (CY13650) carrying the *POL1-6His-3Flag* allele have been released from G1 into 150 mM HU for 60 minutes. Polα binding profiles (light blue), determined by ChIP on chip and relative to the indicated region of the chromosome III are shown. Y-axis shows the signal log2 IP/SUP ratio, which expresses the magnitude of protein-DNA binding in the chromosome *loci* represented (see experimental procedures). Dashed black lines indicate the positions of the early origins *AR305* and *ARS306* and the late origin *ARS316,* which is fired (and bound by Polα) in HU only in checkpoint defective cells.

Rossi et al Supplemental Figure S3

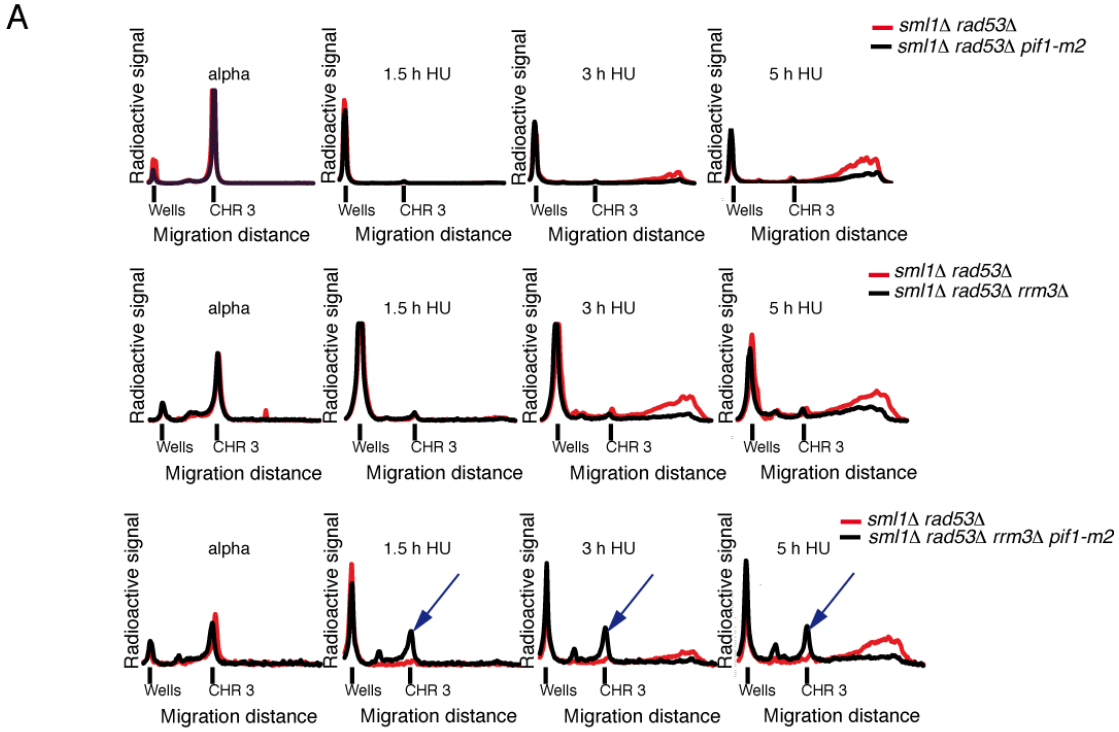

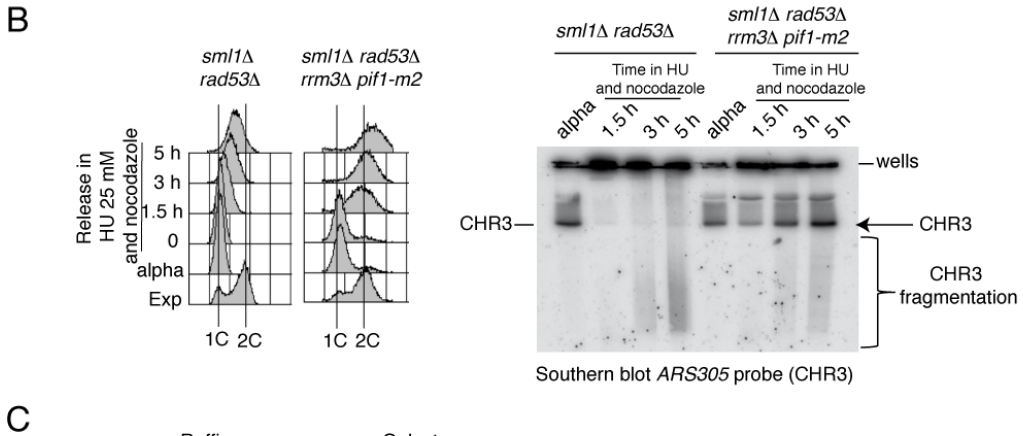

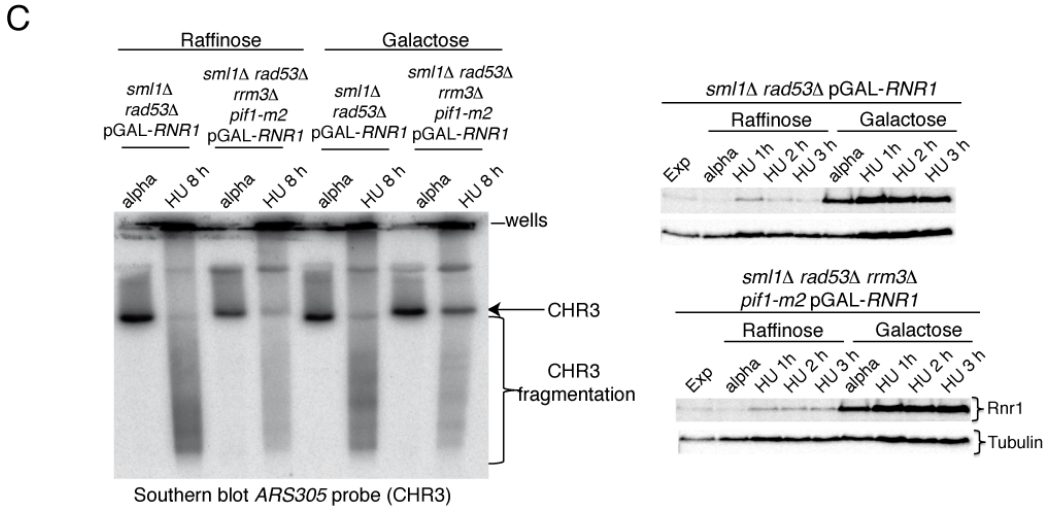

Figure S3. *RRM3* and *PIF1* ablations suppress chromosome fragmentation in *rad53* mutants exposed to replication stress, (related to Figure 3).

A) Quantitative profiles of the PFGE experiments shown in Figure 3 are reported. The intensity of the radioactive signal in each line of the PFGE gels shown in Figure 3 is plotted against the migration distance. In order to quantify and better appreciate the difference in the chromosome fragmentation between different strains, quantitative profiles of the indicated strains analyzed at different time points are overlapped. Blue arrows indicate the signals corresponding to the chromosome III, which re-enters into the gel in the quadruple mutant *sml1Δ rad53Δ rrm3Δ pif1-m2* (CY13342) treated with HU. **B) The ablation of the Pif1 helicases suppresses the chromosome fragmentation observed in *rad53* mutants treated with 25 mM of HU in the first cell cycle.** CY12443 and CY13342 strains were synchronized in G1 and released into S-phase in the presence of 25 mM of HU and nocodazole (20 µg/ml). The migration pattern of chromosome III was analyzed, at the indicated time points, by PFGE and southern blotting, using an *ARS305* recognizing probe. A black arrow indicates the southern blot signal of the chromosome III, which re-enters in the gel in HU only in the strain CY13342. The region of the gel in which chromosome fragmentation is visible is indicated by a black bracket. Position of the wells is shown. FACS profiles with the cellular DNA content during the experiment are shown. **C) High dNTPs levels do not alter the chromosome fragility induced in *rad53* mutants treated with low HU doses.** CY14076 and CY14077 strains, overexpressing the *RNR1* gene under the control of the *GAL1/GAL10* promoter, were released from a G1 arrest into 25 mM of HU for 8 hours, in the presence or absence of galactose. Chromosome III migration pattern has been analyzed by PFGE and southern blotting using an *ARS305* recognizing probe, at the indicated time points. A black arrow indicates the southern blot signal corresponding to the chromosome III, which re-enters in the gel in HU only in the strain CY14077. The region of the gel in which chromosome fragmentation is visible is indicated by a black bracket. Position of the wells is shown. In the lower panel Rnr1 protein levels have been monitored by western blotting, using anti-Rnr1 antibodies and tubulin was used as loading control.

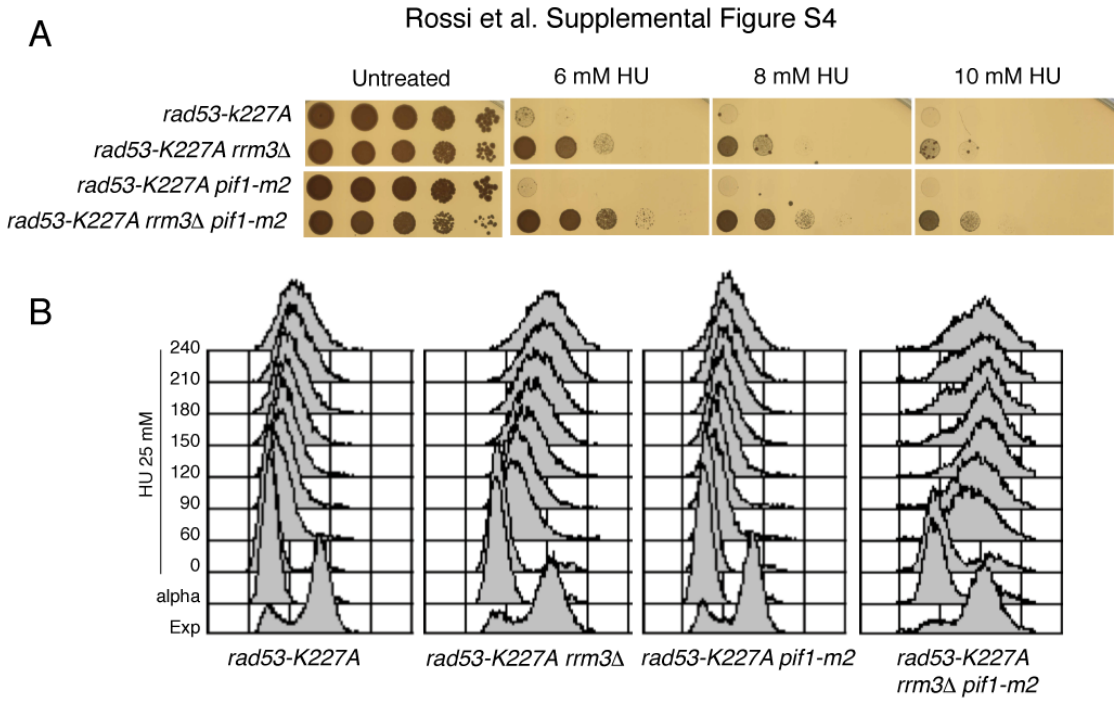

Figure S4. Ablation of the Pif1 helicases suppresses the HU sensitivity and DNA replication forks arrest induced by treatment of *rad53-K227A* mutant cells with low HU doses (related to Figure 4).

A) HU sensitivity of CY12404, CY12406, CY13735 and CY13738 strains has been determined by drop-assay, at the indicated HU dosages. **B)** The same strains as in A have been synchronized in G1 and released into S-phase in the presence of 25 mM of HU. Samples were collected at the indicated time points, and the cellular DNA content has been determined by FACS analysis.

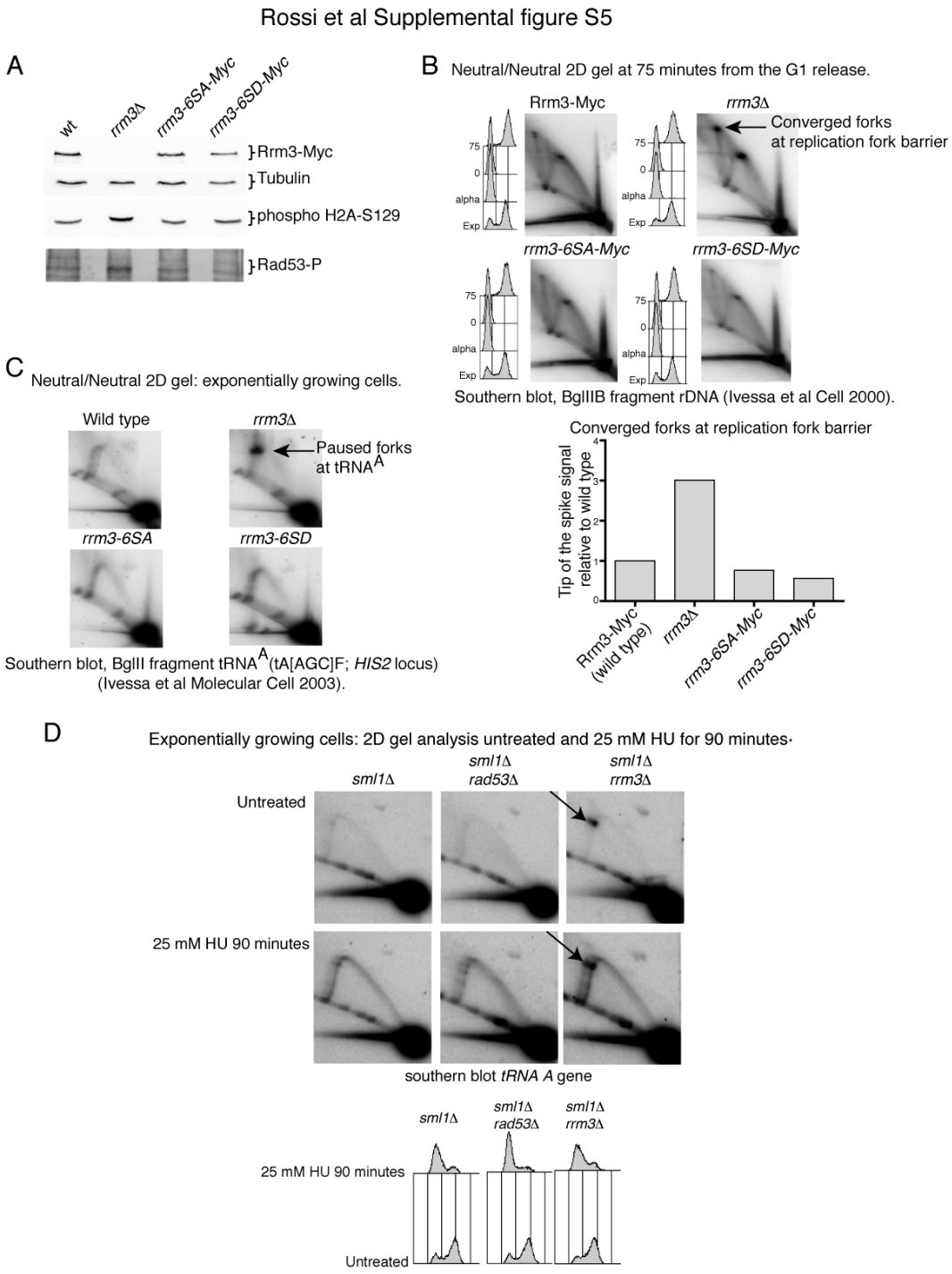

Figure S5. The *rrm3-6SA*, *rrm3-6SD*, *pif1-12A* and *pif1-12D* alleles do not influence protein levels and protein functions in unperturbed conditions, (related to Figure 5). A) The yeast strains *RRM3-13MYC* (CY11360), *rrm3Δ* (CY12484), *rrm3-6SA-13MYC* (CY12803), *rrm3-6SD-13MYC* (CY12831) carrying the indicated *RRM3* alleles have been grown to mid log phase in unperturbed conditions. Protein extracts have been prepared and separated by SDS page. Rrm3 variants, tubuline, histone H2A phosphorylation and Rad53 phosphorylation have been visualized by

western blotting using specific antibodies. **B)** DNA replication intermediates accumulating in the BglIIB fragment of the rDNA (Ivessa et al., 2000), have been visualized through neutral-neutral 2D gel electrophoresis in the yeast strains used in A at 75 minutes from the G1 release in unperturbed conditions. FACS profiles, which show the cellular DNA content during the experiments, are shown. The signals at the tip of the spike arc (corresponding to converged replication forks at the replication fork barrier in the rDNA) (Ivessa et al., 2000), have been normalized against the intensity of their corresponding monomer spots and reported into the histogram as values relative to the wild type signal. **C)** DNA replication intermediates accumulating in the BglII fragment containing the *HIS2* and the $tRNA^{A}$ tA[AGC]F coding region, have been visualized through neutral-neutral 2D gel electrophoresis in the yeast strains wild type (CY12486), *rrm3Δ* (CY12484), *rrm3-6SA*(CY12801) and *rrm3-6SD* (CY12824) grown to mid log phase in unperturbed conditions (Ivessa et al., 2003). **D) Exponentially growing wild type and *rad53Δ* cells do not accumulate DNA replication pausing signals at the *tRNA*^{A} gene even when cells are treated with 25mM of HU for 90 minutes.** CY12445, CY12443 and CY12448 strains were grown to mid log phase and DNA replication intermediates, accumulating on the BglII-*HIS2* restriction fragment containing the *tRNA*^{A} gene, have been analyzed by 2D gel electrophoresis in unperturbed conditions or after 90 minutes of treatment of exponentially growing cells with 25 mM of HU. FACS profiles, which show the cellular DNA content during the experiment, are reported. A black arrow indicates the DNA replication pausing signal induced at the *tRNA*^{A} locus by the absence of *RRM3*.

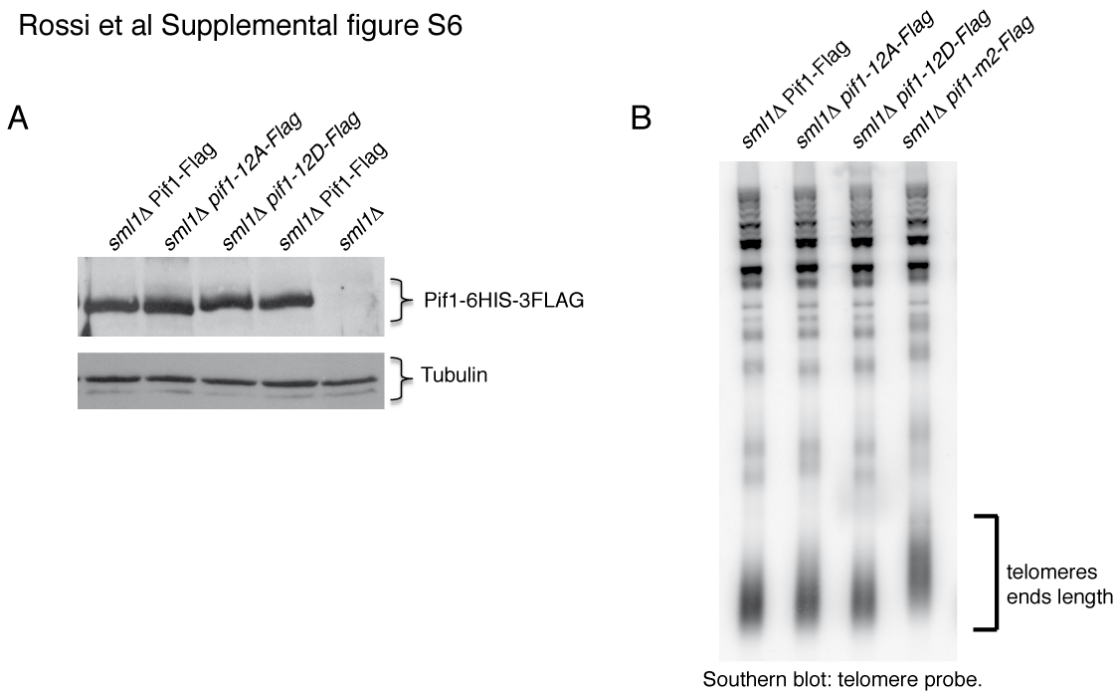

Figure S6 (related to Figure 5).

A) The following yeast strains: *sml1Δ PIF1-6HIS-3FLAG* (CY13074), *sml1Δ pif1-12A-6HIS-3FLAG* (CY13664), *sml1Δ rad53Δ pif1-12D-6HIS-3FLAG* (CY13668), *sml1Δ* (CY12445), have been grown to mid log phase in unperturbed conditions. The protein levels of Pif1-6His-3Flag, *pif1-12A*-6His-3Flag and *pif1-12D*-6His-3Flag and of the tubulin (as loading control), have been analyzed by western blotting, respectively, using anti-flag antibodies and anti tubulin antibodies. **B)** The length of the telomeres has been analyzed by southern blotting using a telomere specific probe as previously described (Longhese et al., 2000) in the yeast strains used in D and in the *sml1Δ pif1-m2-6His-3Flag* strain (CY12934), which have been grown to mid log phase in unperturbed conditions.

Rossi et al. Supplemental Figure S7

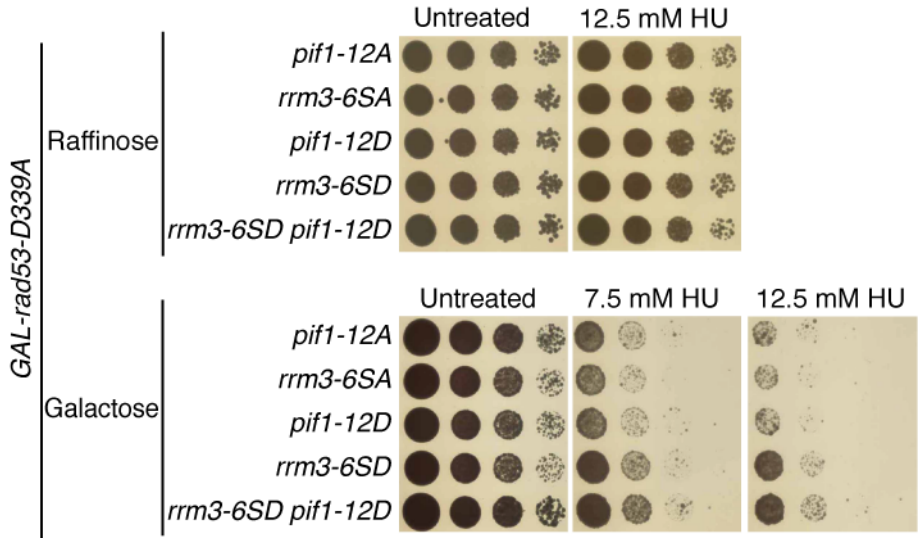

Figure S7 (related to Figure 5).

HU sensitivity has been determined by drop assay at the indicated HU dosages in YP+Raffinose or YP+Raffinose+Galactose in strains: *leu2::2X-LEU2-GAL1-rad53-D339A sml1Δ pif1-12A-6HIS-3FLAG RRM3-13MYC* (CY14011), *leu2::2X-LEU2-GAL1-rad53-D339A sml1Δ Pif1-6HIS-3FLAG rrm3-6SA-13MYC* (CY14013), *leu2::2X-LEU2-GAL1-rad53-D339A sml1Δ pif1-12D-6HIS-3FLAG RRM3-13MYC* (CY14012), *leu2::2X-LEU2-GAL1-rad53-D339A sml1Δ Pif1-6HIS-3FLAG rrm3-6SD-13MYC* (CY14014), *leu2::2X-LEU2-GAL1-rad53-D339A sml1Δ pif1-12D-6HIS-3FLAG rrm3-6SD-13MYC* (CY14015).

Supplemental experimental procedures

Cell were grown in YPD (2% glucose), arrested in alpha factor (4 µg/ml) at 28°C for 2 hours and released with/without HU (25 mM or 150 mM). ChIP on chip experiments were performed and protein-DNA binding profiles generated as described (Bermejo et al., 2009a; Bermejo et al., 2009b) based on the affymetrix platform. PCR amplification steps in our ChIP on chip analysis were carried out under non saturating conditions and the amounts of DNA used to hybridize the affymetrix chips were normalized. The significance of the overlaps between the protein binding clusters and protein binding clusters and BrdU clusters, was evaluated by confrontation against a null hypothesis model generated with a Montecarlo-like simulation, as described (Bermejo et al., 2009a; Bermejo et al., 2009b). The average

binding signals of the indicated proteins at 141 early *ARSs* (Figure 1C), were plotted using the sitepro function in CEAS (Cis-regulatory Element Annotation System) (Shin et al., 2009). We set 50 nt as the profiling resolution and 12,000 nt as the size of flanking regions from the center of each *ARS* (Shin et al., 2009). ssDNA-BrdU IP on chip experiments and profiles has been conducted/generated as described (Katou et al., 2003). Quantitative ChIP-qPCRs using the oligos 305L3F (CCATGACTTTGGCACATCAG) and 305L3R (CGCTGCCTCCTTAGTAATCG) for the strains (CY11360, CY12425, CY12927, CY12698) and the oligos 305L8F (TCAAAGCAGATGCCATGAAC) and 305L8R (CTGTTTGCACGAAGGAATCA) for the strains (CY13074, CY13073, CY13284, CY13282) (see figure 1A-B-D), have been performed as described (Alzu et al., 2012). 2D gel electrophoresis has been conducted on genomic DNA prepared with the C-tab method after sodium azide fixation (40 minutes on ice 0.1% final concentration) and *in-vivo* psoralen cross linking as described (Liberi et al., 2006). PFGE electrophoresis analysis using Amersham gene navigator system has been performed as described (Giannattasio et al., 2010) on sodium azide-treated cellular pellets using the following program: 165V, 23 hours of run with 30 seconds pulses step wise. Phospho-tag gels (7.5%-10% with ratio acrylamide/bis-acrylamide of 75:1 and 40 μM of P-tag reagent) has been prepared according to manufacturer instructions (Kinoshita et al., 2006). Analysis of replication forks by trasmission electron microscopy has been performed as described (Neelsen et al., 2014). All the strains used in this study are listed in Table S1 and are W303 derivatives with the wild type *RAD5* locus. The *rrm3* and *pif1* alleles have been generated using the "delitto perfetto" strategy (Storici and Resnick, 2006). Mutant alleles expressing fusion proteins with different tags have been generated by one step replacement systems using different template plasmids as described (Longtine et al., 1998).

Supplemental references

Alzu, A., Bermejo, R., Begnis, M., Lucca, C., Piccini, D., Carotenuto, W., Saponaro, M., Brambati, A., Cocito, A., Foiani, M., *et al.* (2012). Senataxin Associates with Replication Forks to Protect Fork Integrity across RNA-Polymerase-II-Transcribed Genes. Cell *151*, 835-846.

Bermejo, R., Capra, T., Gonzalez-Huici, V., Fachinetti, D., Cocito, A., Natoli, G., Katou, Y., Mori, H., Kurokawa, K., Shirahige, K., *et al.* (2009a). Genome-organizing

factors Top2 and Hmo1 prevent chromosome fragility at sites of S phase transcription. Cell *138*, 870-884.
Bermejo, R., Katou, Y.M., Shirahige, K., and Foiani, M. (2009b). ChIP-on-chip analysis of DNA topoisomerases. Methods in molecular biology *582*, 103-118.
Giannattasio, M., Follonier, C., Tourriere, H., Puddu, F., Lazzaro, F., Pasero, P., Lopes, M., Plevani, P., and Muzi-Falconi, M. (2010). Exo1 competes with repair synthesis, converts NER intermediates to long ssDNA gaps, and promotes checkpoint activation. Mol Cell *40*, 50-62.
Ivessa, A.S., Lenzmeier, B.A., Bessler, J.B., Goudsouzian, L.K., Schnakenberg, S.L., and Zakian, V.A. (2003). The Saccharomyces cerevisiae helicase Rrm3p facilitates replication past nonhistone protein-DNA complexes. Mol Cell *12*, 1525-1536.
Ivessa, A.S., Zhou, J.Q., and Zakian, V.A. (2000). The Saccharomyces Pif1p DNA helicase and the highly related Rrm3p have opposite effects on replication fork progression in ribosomal DNA. Cell *100*, 479-489.
Kinoshita, E., Kinoshita-Kikuta, E., Takiyama, K., and Koike, T. (2006). Phosphate-binding tag, a new tool to visualize phosphorylated proteins. Molecular & cellular proteomics : MCP *5*, 749-757.
Liberi, G., Cotta-Ramusino, C., Lopes, M., Sogo, J., Conti, C., Bensimon, A., and Foiani, M. (2006). Methods to study replication fork collapse in budding yeast. Methods in enzymology *409*, 442-462.
Longhese, M.P., Paciotti, V., Neecke, H., and Lucchini, G. (2000). Checkpoint proteins influence telomeric silencing and length maintenance in budding yeast. Genetics *155*, 1577-1591.
Longtine, M.S., McKenzie, A., 3rd, Demarini, D.J., Shah, N.G., Wach, A., Brachat, A., Philippsen, P., and Pringle, J.R. (1998). Additional modules for versatile and economical PCR-based gene deletion and modification in Saccharomyces cerevisiae. Yeast *14*, 953-961.
Neelsen, K.J., Chaudhuri, A.R., Follonier, C., Herrador, R., and Lopes, M. (2014). Visualization and interpretation of eukaryotic DNA replication intermediates in vivo by electron microscopy. Methods in molecular biology *1094*, 177-208.
Shin, H., Liu, T., Manrai, A.K., and Liu, X.S. (2009). CEAS: cis-regulatory element annotation system. Bioinformatics *25*, 2605-2606.
Storici, F., and Resnick, M.A. (2006). The delitto perfetto approach to in vivo site-directed mutagenesis and chromosome rearrangements with synthetic oligonucleotides in yeast. Methods in enzymology *409*, 329-345.